Electronic Supplementary Material (ESI) for Inorganic Chemistry Frontiers.

Supporting information

Fabrication of redox-active polyoxometalates-based ionic crystals onto single-walled carbon nanotubes for high-performance anode materials of lithium-ion batteries

Bushra Iqbal, Xueying Jia, Hanbin Hu, Lei He*, Wei Chen, and Yu-Fei Song*

State Key Laboratory of Chemical Resource Engineering, Beijing Advanced Innovation Center for Soft Matter Science and Engineering, Beijing University of Chemical Technology, Beijing 100029 P. R. China.

*E-mail: songyf@mail.buct.edu.cn, helei@mail.buct.edu.cn; Tel/Fax: +86 10-64411832.

List of contents:

Figure S1. FT-IR spectra of $PMo_{12}O_{40}$, Co_3 cluster, and Composite 1, respectively.

Figure S2. Raman spectra of $PMo_{12}O_{40}$

Figure S3. XRD spectra of Composite 1, SWNTs, and Composite 1/SWNTs nanocomposite

Figure S4. HRTEM-EDX pattern of Composite 1/SWNTs nanocomposite

Figure S5. Electrochemical performance of the Composite 1

Figure S6. Nyquist plots of Composite 1, $PMo_{12}O_{40,}$ and Co_3 cluster. (Inserted) The simulated equivalent circuit model of the electrode/electrolyte interface.

Table S1. Comparison of different anode materials and their LIBs performance.

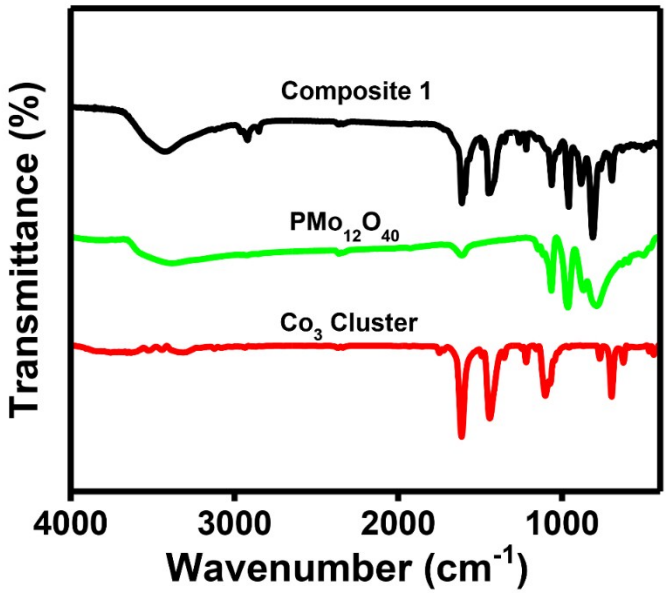

Figure S1. FT-IR spectra of $PMo_{12}O_{40}$, Co_3 cluster, and Composite 1, respectively.

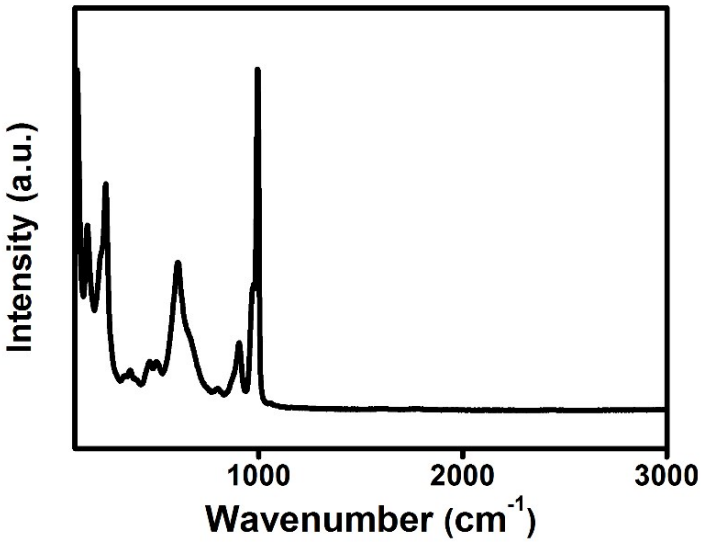

Fig. S2. Raman spectra of $PMo_{12}O_{40}$.

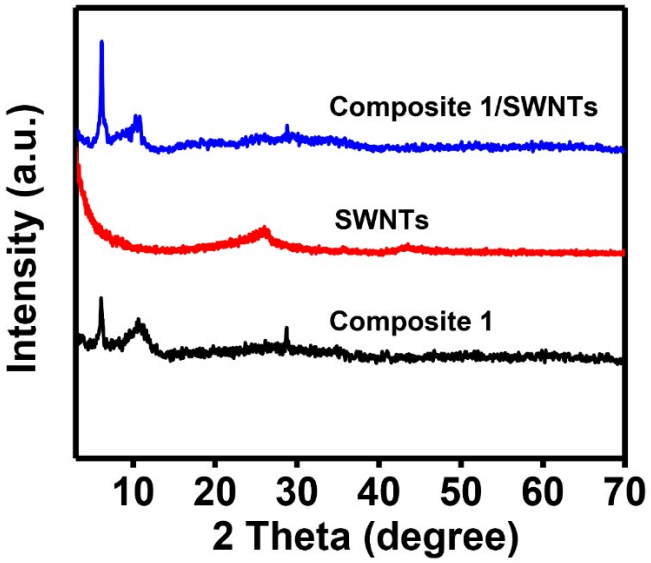

Figure S3. XRD spectra of Composite 1, SWNTs, and Composite 1/SWNTs nanocomposite.

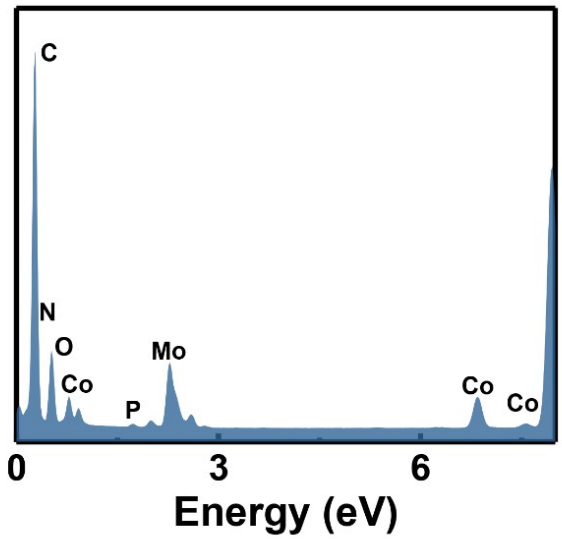

Figure S4. HRTEM-EDX pattern of Composite 1/SWNTs nanocomposite.

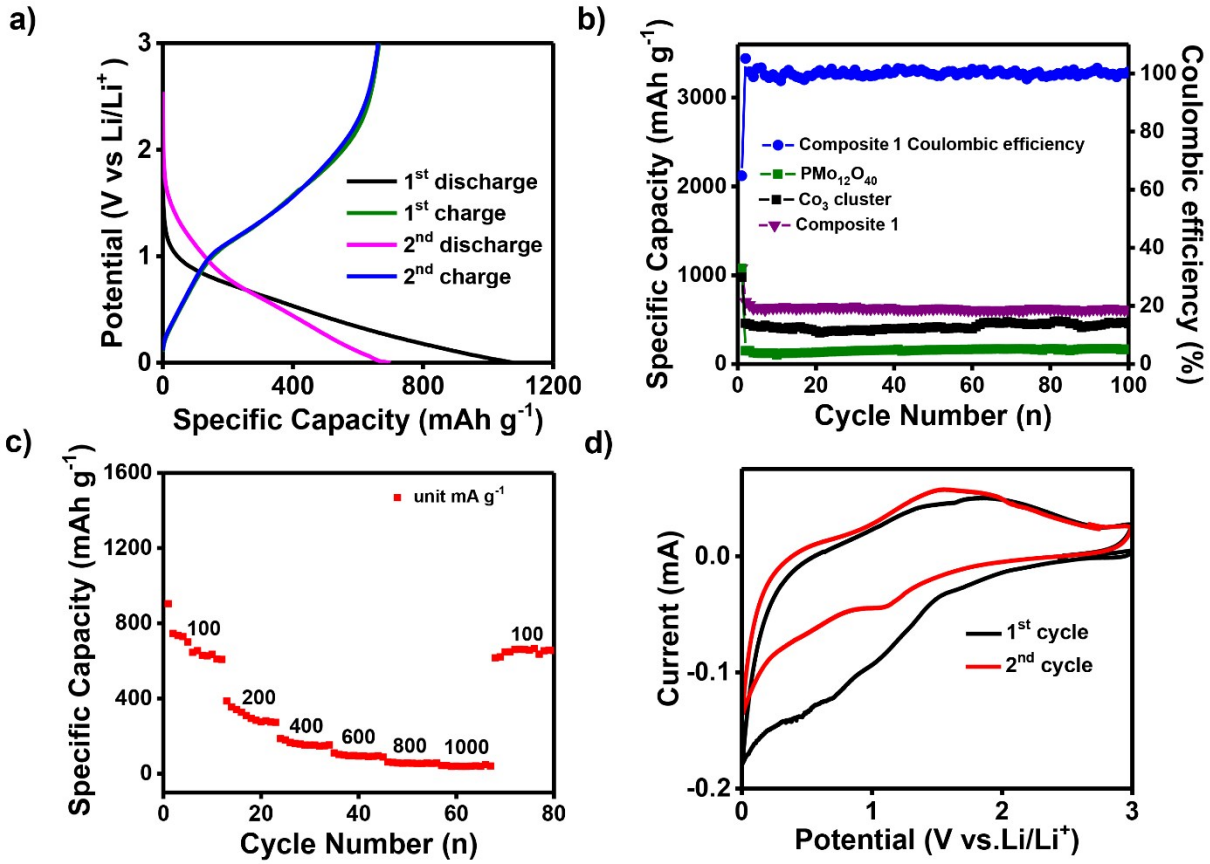

Figure S5. (a) The discharge/charge curves of the Composite 1 at 100 mA g^{-1}, (b) cyclic performance of Composite 1, $PMo_{12}O_{40}$ and Co_3 cluster, (c) rate capability of Composite 1, and (d) CV of Composite 1 at a scan rate of 0.1 mV s^{-1} within 0-3 V.

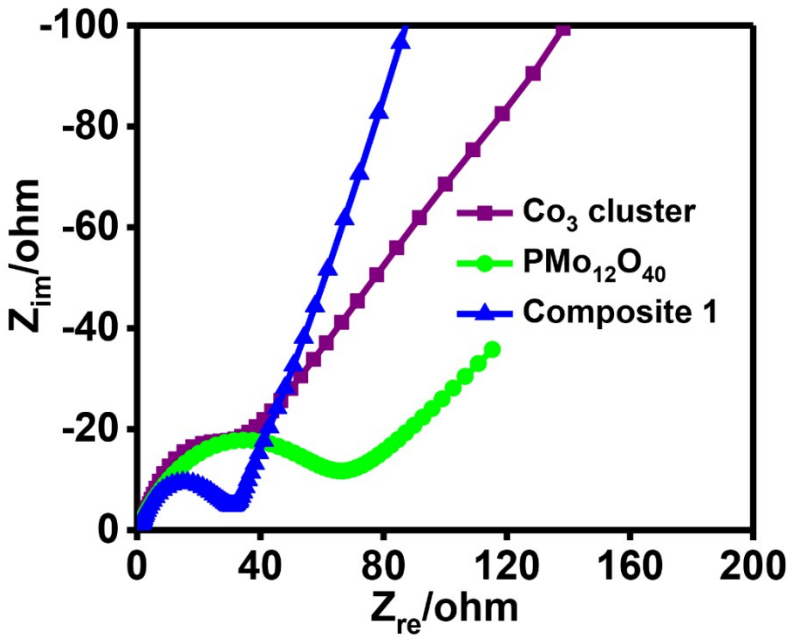

Figure S6. Nyquist plots of Composite 1, $PMo_{12}O_{40}$, and Co_3 cluster. (Inserted) The simulated equivalent circuit model of the electrode/electrolyte interface.

Table S1. Comparison of different anode materials and their LIBs performance

Electrode Materials	**Current density**	**Reversible capacity (cycle times) /mAh g^{-1}**	**Ref.**
$PMo_{10}V_2$/PDA	100 mA g^{-1}	915.3 (63)	[1]
TBA-$PMo_{11}V$/CNTs	0.5 mA cm^{-2}	850 (100)	[2]
CNTs–SiW_{11}	0.2 mA cm^{-2}	650 (100)	[3]
SWNT-sFe_3O_4/CMC	450 mAg^{-1}	687 (100)	[4]
p-SWNT/GNS	200 mAg^{-1}		[5]
N-carbon/rGO	0.1 mAg^{-1}	669 (200)	[6]
Py-Anderson-CNTs	0.5 $mAcm^{-2}$	665.3 (100)	[7]
GO-IL-P_2Mo_{18}	100 mAg^{-1}	973 (100)	[8]
GQD/metal oxide composites	100 mAg^{-1}	970 (100)	[9]
TBA_4[Py-SiW_{11}]-SWNTs	0.5 $mAcm^{-2}$	580 (100)	[10]
PMo_{12}−PPy/RGO	100 mAg^{-1}	1000 (50)	[11]
Composite 1/SWNTs	100 mAg^{-1}	1012 (100)	This work

References:

1 Y.-H. Ding, J. Peng, S.-U. Khan and Y. Yuan, A new polyoxometalate (POM)-based composite: fabrication through POM-assisted polymerization of dopamine and properties as anode materials for high-performance lithium-ion batteries, *Chem. Eur. J.*, 2017, **23**, 10338-10343.

2 J. Hu, Y. Ji, W. Chen, C. Streb and Y.-F. Song, "Wiring" redox-active polyoxometalates to carbon nanotubes using a sonication-driven periodic functionalization strategy, *Energy Environ. Sci.*, 2016, **9**, 1095-1101.

3 W. Chen, L. Huang, J. Hu, T. Li, F. Jia and Y.-F. Song, Connecting carbon nanotubes to polyoxometalate clusters for engineering high-performance anode materials, *Phys. Chem. Chem. Phys.*, 2014, **16**, 19668-19673.

4 Y. H. Kwon, K. Minnici, J. J. Park, S. R. Lee, G. Zhang, E. S. Takeuchi, K. J. Takeuchi, A. C. Marschilok and E. Reichmanis, SWNT anchored with carboxylated polythiophene "links" on high-capacity Li-ion battery anode materials, *J. Am. Chem. Soc.*, 2018, **140**, 5666-5669.

5 H. Kim, J. Kim, H. Jeong, H. Kim, H. Lee, J.-M. Ha, S.-M. Choi, T.-H. Kim, Y.-C. Nah, T. J. Shin, J. Bang, S. K. Satija and J. Koo, Spontaneous hybrids of graphene and carbon nanotube arrays at the liquid-gas interface for Li-ion battery anodes, *Chem. Commun.*, 2018, **54**, 5229-5232.

6 X. Liu, J. Zhang, S. Guo and N. Pinna, Graphene/N-doped carbon sandwiched nanosheets with ultrahigh nitrogen doping for boosting lithium-ion batteries, *J. Mater. Chem. A*, 2016, **4**, 1423-1431.

7 L. Huang, J. Hu, Y. Ji, C. Streb and Y.-F. Song, Pyrene-Anderson-modified CNTs as anode materials for lithium-ion batteries, *Chem. Eur. J.*, 2015, **21**, 18799-18804.

8 J. Hu, H. Diao, W. Luo and Y.-F. Song, Dawson-Type polyoxomolybdate anions ($P_2Mo_{18}O_{62}^{6-}$) captured by ionic liquid on graphene oxide as high-capacity anode material for lithium-ion batteries, *Chem. Eur. J.*, 2017, **23**, 8729-8735.

9 Y. Ji, J. Hu, J. Biskupek, U. Kaiser, Y.-F. Song and C. Streb, Polyoxometalate-based bottom-up fabrication of graphene quantum dot/manganese vanadate composites as lithium ion battery anodes, *Chem. Eur. J.*, 2017, **23**, 16637-16643.

10 D. Ma, L. Liang, W. Chen, H. Liu and Y.-F. Song, Covalently tethered polyoxometalate-pyrene hybrids for noncovalent sidewall functionalization of single-walled carbon nanotubes as high-performance anode material, *Adv. Funct. Mater.*, 2013, **23**, 6100-6105.

11 M. Zhang, T. Wei, A.-M. Zhang, S.-L. Li, F.-C. Shen, L.-Z. Dong, D.-S. Li and Y.-Q. Lan, Polyoxomolybdate-polypyrrole/reduced graphene oxide nanocomposite as high-capacity electrodes for lithium storage, *ACS Omega*, 2017, **2**, 5684-5690.